Seismic Response of Multi-Story Structure Strengthened with Micropiles

Noha El-Shamy, Sayed M. Ahmed, M. A. Abdel-Motaal

Abstract: ***Micropiles are reinforced grouted piles that have small diameters commonly not higher than 30 cm. They are widely used for slope stabilization, controlling structural settlement, and in some cases, as retaining structures. Also, they are used for resisting dynamic uplift loads, seismic retrofit mainly in restrictive and low headroom areas, and retrofitting of historical monuments. The main goal of this research is to develop a finite element model that can capture the different aspects of seismic behavior of multi-story structure supported with deep foundation via using of micropiles. Also, a main target for the executing numerical modelling is to show the influence of the surrounding soil on this system and vice versa. Firstly, a representative two-dimensional finite element model is conducted to represent the soil-structure interaction system under seismic excitation supported with proper boundary conditions in PLAXIS 2D V20 for dynamic analysis based on previous recommendations considering the nonlinear soil behavior. The behavior of micropiles is studied and verified using previous results. Based on these models, the effect of lateral dynamic loads on the response of a structure with different foundation types is investigated. Also, a wide range of parametric studies, considering structure properties, earthquake magnitude, micropile diameter, micropile length, and the number of micropiles, have been carried out in order to investigate the actual interaction between soil, sub-structure, and superstructures. The study results showed that the seismic response of the structure is highly affected by the properties of the sub-surface soil layer. Consequently and similarly, analysis results established that underpinning using micropiles is an efficient technique for controlling the seismic response of existing structures.***

Keywords: ***Dynamic Soil-Structure Interaction, Micropiles Underpinning, Multi-Story Building, Nonlinear Analysis, Response Spectrum, Seismic Excitation.***

I. INTRODUCTION

Earthquakes can be described as a sudden strong ground shaking resulting in damages and deaths as a result of strong shaking and fault rupture. This shaking may last from seconds to minutes. The resulting damages from earthquakes are divided into primary and secondary damages. Structural damage is classified as the most primary and dramatic image of earthquake damages. It differs in intensity according to the frequency of the motion, earthquake magnitude, and source of the earthquake. Secondary damage is the consequence events of the strong shaking as this shaking may induce excessive settlement or lateral spreading due to loss of soil stiffness 1.

Deep foundations, including pile and micropile foundations, are used excessively for load transfer in various structures types such as multi-story towers and offshore structures. Previously, pile foundations were designed mainly to support axial loads only while the loading condition in case of earthquake excitation transfers lateral forces and moments to the piles. Earthquakes are not the only type of dynamic lateral loading that can affect pile foundations, but there are other types such as wind load, braking forces from moving vehicles in bridge abutments cases, and water action on offshore structures 2. Meyersohn 3 and Bhattacharya 4 illustrated the impact of these lateral loads on pile foundations design. They suggested two modes of failures for laterally loaded piles. One of them is the buckling mode, which is significantly affected by pile length through liquefied soil. The other mode is called bending mode due to soil deformation, which results in high deformation of pile till reaching its moment of resistance. This soil deformation occurs at high values due to nonlinear soil behavior. These nonlinear soil characteristics are determined as one of the most effective factors on the magnitude of the dynamic soil effects 1 5 6. Micropiles are reinforced piles that have small diameters commonly not higher than 30 cm. They should be well grouted, as they are designed to transfer loads mainly by skin friction. Micropiles are used in active seismic zones for structures rehabilitation or in new constructions as they exhibit a good performance in seismic conditions. Nowadays, there is a great interest in micropiles because:

a) They are easily installed in access-restrictive sites and almost in all soil types.

b) They are flexible in cases of seismic conditions because of their ability to resist extension forces as the higher percentage of micropiles capacity is derived from the steel reinforcement.

c) Inclined micropiles are installed easily. It's noteworthy to mention that inclined micropiles have a positive effect under seismic conditions 7.

II. LITERATURE

The most common methods that are used in the earlier researches to study the dynamic response of laterally loaded micropiles are: Winkler approach, P-Y curves, and finite element method.

Revised Manuscript Received on August 15, 2020.
* Correspondence Author

Noha El-Shamy*, Department of Civil Engineering, Ain Shams University, Cairo, Egypt. E-mail: noha12095@eng.asu.edu.eg

Sayed M. Ahmed, Department of Civil Engineering, Ain Shams University, Cairo, Egypt. E-mail: Sayed_mohamed@eng.asu.edu.eg

M. A. Abdel-Motaal, Department of Civil Engineering, Ain Shams University, Cairo, Egypt. E-mail: abdelmotal@yahoo.com

Winkler method depends on the subgrade reaction coefficient; the soil is represented by a group of linear springs with a stiffness equal to soil Young's modulus. Resse 8 defined this stiffness with ($E_s = \frac{p}{y}$), where P is the lateral soil reaction per pile unit length in force/length units (F/L), and y is the pile's lateral deflection in the opposite direction to soil reaction direction.

P-Y curves method is thought to be an extension of the Winkler method. McClelland and Focht 9 invented the p-y method to overcome the limitations of the Winkler model. Soil is represented by a group of nonlinear springs and piles with beam elements. A group of p-y curves is utilized to represent the soil reaction in nonlinear behavior. The most prominent formulation of p-y curves is the cubic parabola formula $\frac{p}{p_{ult}} = 0.5\left(\frac{y}{y_{50}}\right)^{0.33}$, where p_{ult} is the ultimate soil pressure per pile unit length, and y_{50} is the pile's lateral deflection at half the ultimate soil pressure capacity. Although the p-y curves method had become widespread, it has some shortcomings, such as it is still considered semi-empirical expression about what happened in nature and that the presentation of soil by p-y curves does not show its continuity along the pile length 10.

Finite Element (FE) method provides the most flexible and acceptable tool for understanding piles' seismic response 11,12. Using finite element modeling, Juran et al. 13 conducted a 3D FE model and centrifuge model test to study the seismic performance of micropiles and the influence of some main parameters on the seismic behavior of micropiles. Results showed that during seismic loading, micropiles follow the soil movement closely. Also, the use of micropiles in a group was studied, and it led to a good increase in the stiffness of the foundation and a decrease in bending moment and shear forces induced by seismic loads.

Souli and Shahrour 14 studied the elastic and elastoplastic behavior of the soil-structure-micropiles system. It was concluded that pure elastic analysis led to an overestimation of the axial component and underestimation of the bending moment. Ghorbani et al. 15 investigated the influence of most of the essential parameters on micropiles' performance by executing a 3-D finite element model. This study listed amplitude of earthquake, number of micropiles, slenderness ratio, and mass of the superstructure as the most influential parameters on the resulting micropiles' deformations and maximum stresses, respectively.

Alfach 16 conducted a numerical simulation for a problem of strengthening of a piled bridge with micropiles. The results approved the efficiency of system reinforcement with micropiles. Results also revealed a positive effect of micropiles inclination and small pile-micropile spacing on the internal forces in piles and micropiles themselves.

Mashhoud et al. 17 conducted shaking table tests as well as finite element modeling by ABAQUS on vertical and inclined groups of micropiles existed in the sand of low relative density. Main study observations recorded an increase in acceleration values through soil layers, an increase in bending moment values at the corner piles than center piles, and a decrease in bending moment values considering the inclined micropiles group.

This paper performs a detailed seismic analysis of multi-story structure, first using shallow foundation and then after strengthening using micropiles. Numerical analysis is done using the FE program PLAXIS 2D V20. Previous work has used some simplifications, such as neglecting simulation of the superstructure. Therefore, the superstructure is fully modeled to study the mutual effect between superstructure, underneath soil, and micropiles to achieve more reliable results. Previous researchers such as Benz 18 and R. Obrzud 19 concluded that the hardening soil model with small-strain stiffness (HS-Small) is essential to simulate the surrounding soil's nonlinear behavior, especially in engineering problems with unloading-reloading paths. Therefore, the HS-Small model is adopted in the present research.

Effects of foundation type, soil properties, micropiles distribution, micropiles properties, and superstructure properties on the seismic response of structures with micropiles foundations have been studied to investigate their effect on the seismic interaction in terms of:

a) Structure's fundamental periodic time.
b) Free field acceleration change.
c) Overall displacement.
d) Induced piles' bending moment.

III. NUMERICAL MODELING

A. Hardening Soil Model with Small-Strain Stiffness

The chief advantage of HS-small model is that the variation of soil stiffness depending on strain amplitudes is correctly modeled by considering two additional master parameters over hardening soil model parameters:

1- Small strain shear modulus (also known as initial modulus) G_o^{ref} at a reference confining stress $\sigma_3 = P_{ref}$.
2- Shear strain threshold ($\gamma_{0.7}$), which expresses a reduction from the initial modulus in the secant shear modulus to about 70% (accurately to 72.2%). Fig.1 shows the modulus reduction curve that explains the influence of different shear strain levels on soil shear modulus 1 20.

Many correlations are developed to evaluate the maximum initial shear modulus depending on soil's properties as void ratio, plasticity index, effective stresses, …etc. Hardin & Black 21 suggested a correlation to estimate $\boldsymbol{G_0^{ref}}$ in various soils with natural void ratio, by the following relationship (1) for crushed sands and undisturbed clayey soils.

$$G_0^{ref} = 33\frac{(2.97-e)^2}{1+e} \text{ in } [MPa] \quad (1)$$

Since it is difficult to assess an accurate value for the threshold shear strain $\gamma_{0.7}$, it can be estimated from the well-known curves established before as Vucetic & Dobry chart 20 shown in Fig.2, noting that cohesionless soils are soils with zero plasticity (P.I = 0).

Retrieval Number: F1511089620/2020©BEIESP
DOI: 10.35940/ijeat.F1511.089620
Journal Website: www.ijeat.org

Published By:
Blue Eyes Intelligence Engineering
and Sciences Publication

International Journal of Engineering and Advanced Technology (IJEAT)
ISSN: 2249-8958 (Online), Volume-9 Issue-6, August 2020

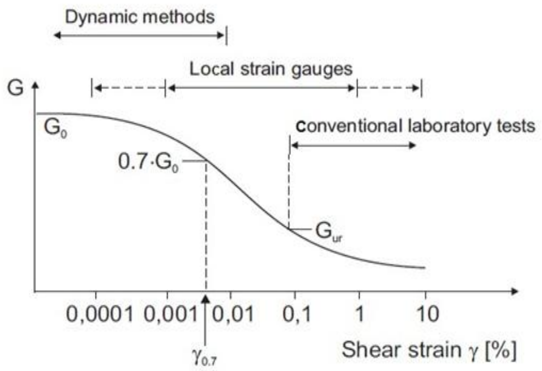

Fig.1: The effect of different shear strain rates on soil shear modulus. (Atkinson & Sallfors, 1991)

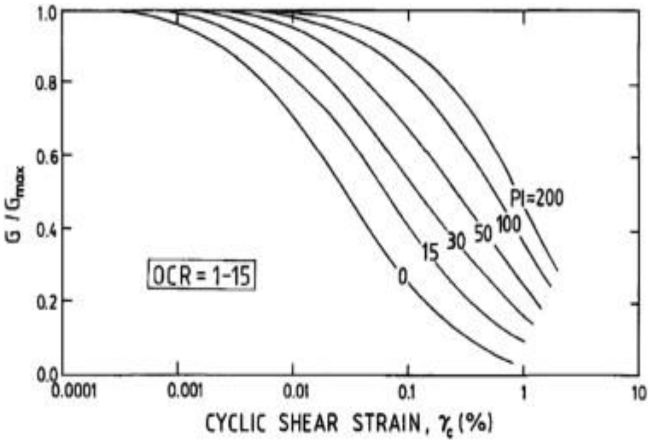

Fig.2: Variation of soil backbone curves with respect to soil plasticity. (Vucetic & Dobry, 1991)

B. Damping Properties

Typically, the energy of vibration diminishes in amplitude with time due to some properties depending on material type and source of vibration, which is called the damping process 22. Damping is represented in numerical modeling by various mechanisms. Radiation damping is achieved in the model by one of the following two options; damping the waves with material damping during travel towards the model boundary or by using full absorbent boundaries to control wave reflection. In the finite element models, the prevention of waves' radiation cannot be accomplished by defining the boundaries too far away for computational convenience. Instead, artificial small Rayleigh material damping, in combination with far absorbing boundaries are introduced to present the required attenuation of stress waves at the field by radiation damping. Relaxation coefficients C_1 and C_2 are applied to improve the absorption quality at the boundaries. In cases of earthquakes, the primary waves are the shear waves, So C_1=1 while C_2 factor is studied to express the required attenuation of waves for the chosen boundaries 23.

Although material damping is ensured within using HS-SMALL material model, Rayleigh damping coefficients should be introduced from (2) & (3) to implement small damping ratio suggested being with an approximate value around 0.5-2% to represent the energy dissipation at very small shear strains where hysteretic damping function of soil model is clarified at shear strains larger than about 10^{-6} 24.

$$[C] = \alpha[M] + \beta[K] \tag{2}$$

$$\alpha = \frac{2\,\xi\omega_i\omega_j}{\omega_i + \omega_j},$$
$$\beta = \frac{2\,\xi}{\omega_i + \omega_j} \tag{3}$$

Where [C] is the material damping matrix for the system, [M] & [K] are the mass and stiffness matrices for the system, respectively.

C. Boundary Conditions

Many researchers studied different boundary conditions used for dynamic analysis, such as Magar 25 and Toma 12. Based on the boundary condition test by Magar 25, a fixed base which presents the standard fixities in the vertical direction tied degree of freedom, and free lateral boundaries are determined as the most feasible boundaries for dynamic analysis in a plane-symmetric model compared its results with analytical solution results. The boundary relaxation coefficient C_2 is adjusted to 0.25 to improve the waves' absorption. A simple homogeneous linear elastic material is utilized to simplify the estimation of soil parameters with thickness 25 m and shear velocity with 300 m/sec, which gives natural soil frequency 3 Hz. Boundary conditions and damping factors to get 5% damping is selected as explained before. The model is shaken using lateral waves with different frequencies for a harmonic acceleration value 0.1g.

The amplification in acceleration is determined from the PLAXIS model with the ratio between maximum absolute acceleration at the surface of the soil layer and maximum acceleration at bedrock. This factor is compared to the theoretical amplification factor calculated from Kramer 1 as illustrated in (4) where v_s is the shear wave velocity, ω is the natural frequency, H is the thickness for the soil layer, and ξ is the required soil damping. The results illustrated in Fig.3 show a satisfactory agreement, which indicates that the chosen boundaries can attain good performance.

$$F_\omega = \frac{\text{max. acceleration at ground surface}}{\text{max. acceleration at bedrock}}$$
$$= \frac{1}{\sqrt{\cos^2\left(\frac{\omega.H}{v_s}\right) + \left[\xi\left(\frac{\omega.H}{v_s}\right)\right]^2}} \tag{4}$$

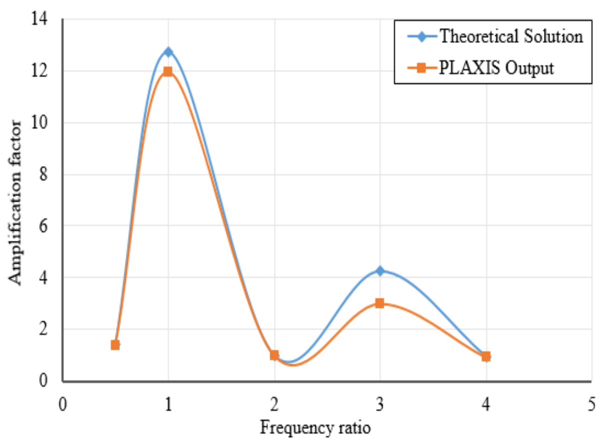

Fig.3: Relationship between amplification factor and frequency ratio.

IV. SOIL AND MICROPILE PARAMETERS VERIFICATION

Retrieval Number: F1511089620/2020©BEIESP
DOI: 10.35940/ijeat.F1511.089620
Journal Website: www.ijeat.org

Published By:
Blue Eyes Intelligence Engineering
and Sciences Publication

An existing four-story building in Al-Zamalek District, Great Cairo, Egypt was studied. The existing superstructure consists of four floors of a reinforced concrete skeleton, and it is intended to raise this building to ten aboveground floors (adding 6 floors). The existing foundation system is a concrete raft of 70 cm thickness. The proposal for strengthening the foundation will be based on adding micropiles as it is regarded as the best solution in this case because the advantage of driving micropiles under existing buildings in a limited area and without harm for the neighboring buildings. Four boreholes at depths with ranges between 25 and 30 meters were conducted in the site to present the geotechnical data and the properties of the sub-soil formations. The results of the SPT test with depth for the boreholes are seen in Fig.4.

A micro-pile load test was implemented on a non-working micropile with a diameter of 25 cm, and length equals 21 m to ensure the bearing capacity of the suggested micropiles. The micropile was tested to a load of 1200 KN, which equals three times its estimated working capacity.

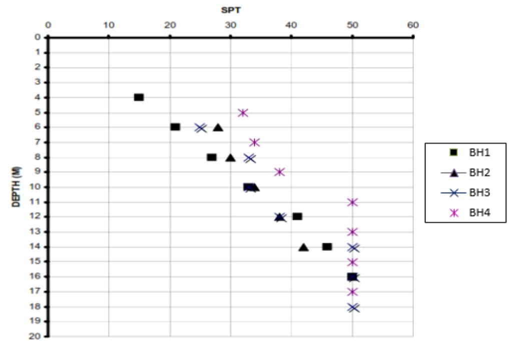

Fig.4: SPT test results with depth for the boreholes.

A PLAXIS-2D model (Fig.5) simulated this pile load test by applying incremental loads for a determinate time. The pile was modeled with a 250 mm diameter embedded beam row element. Equivalent Young's modulus for pile section is used with an average value of 3.8E+7 kPa to consider the steel stiffness as the micropile reinforcement is 3 bars of 32 mm diameter with reinforcement ratio around 5%. According to Boreholes log and SPT results, the stratigraphy of soil layers with their main parameters used in the analysis can be summarized in Table-I.

Table-I: Summary of the used soil properties

Parameter	Symbol (Unit)	Clayey SILT and SAND	Silty Sand	Dense Sand
Layer thickness	h (m)	6	6	48
Saturated soil unit weight	$\gamma_{sat}\ (KN/m^3)$	18	18	20
Unsaturated soil unit weight	$\gamma_{unsat}\ (KN/m^3)$	15	18	20
Reference secant stiffness (triaxial test)	$E_{50}^{ref}\ (MPa)$	30	50	100
Reference tangent stiffness (oedometer test)	$E_{oed}^{ref}\ (MPa)$	30	50	100
Unloading/reloading stiffness	$E_{ur}^{ref}\ (MPa)$	120	200	300
Stress level dependency factor	m	0.7	0.7	0.5
Friction angle	$\varphi^{/}$	22	33	38
Shear strain threshold at 0.722 G_o	$\gamma_{0.7}$	1E-4	3e-4	8E-4
Maximum shear modulus	$G_0^{ref}(MPa)$	100	150	250
Unloading/reloading Poisson's ratio	υ_{ur}	0.2	0.2	0.2
Reference pre-consolidation Pressure	$P^{ref}(KPa)$	12	32	129
Earth pressure coefficient at rest	k_o	0.5	0.455	0.384

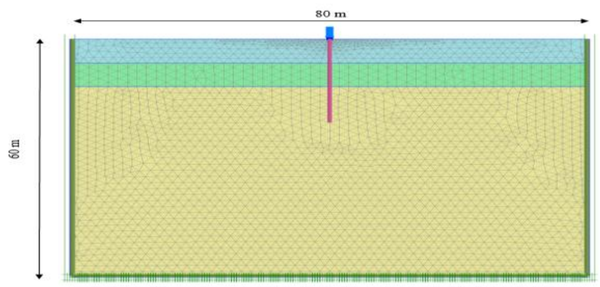

Fig.5: PLAXIS 2D model of micropile load test.

Figure 6 shows the measured and calculated load-settlement curves at the micropile head, which show an acceptable agreement of results. The results validate the estimated soil properties and the modeling of piles with the embedded beam row feature.

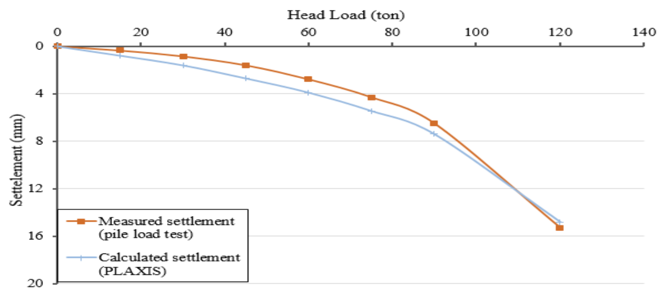

Fig.6: Load settlement curve for a non-working micropile.

V. DYNAMIC SOIL-STRUCTURE-MICROPILES BEHAVIOR

A. Foundation type

This section aims to study the impact of foundation types on the seismic response of the structure. The study extends to discuss the effect of foundation underpinning using micropiles. On the principal case of the building with 4 stories, four foundation types were modeled to evaluate the effect of foundation type on the seismic performance of the building. The structure is presented by considering the middle span of the building. Slabs, columns, and tie beams are modeled with plate elements with an elastic isotropic material model, while footings are modeled with linear elastic soil block with reinforced concrete properties. The four types respectively are:

1- Square isolated footings with dimensions of 200 x 200 x 70 cm.
2- Square isolated footings with dimensions of 200 x 200 x 70 cm connected with ties 20x70cm.
3- Raft with thickness 70 cm.
4- Raft with thickness 70 cm with micropiles (L=21 m, D=25 cm, and number in the mid-span = 18). For example, the finite element model of the structure rested on a raft with micropiles is illustrated in Fig.7.

Earthquake excitation is implemented using seismic central motion at the model bedrock level. Artificial earthquake time history GEQ II by Abdel-Motaal 26, Fig.8, is used after scaling to simulate the target earthquake intensity or maximum acceleration.

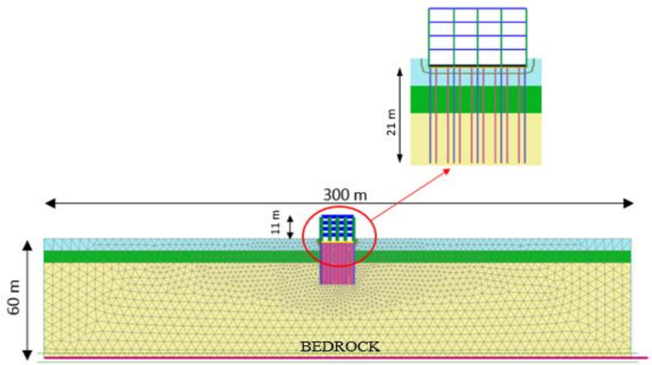

Fig.7: Finite element model of the structure rested on raft with micropiles.

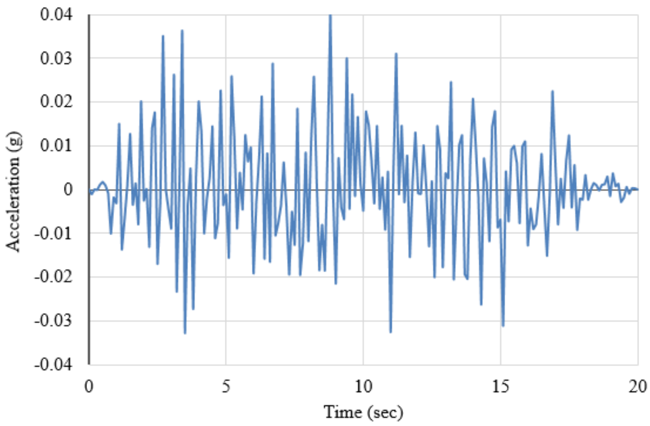

Fig.8: Time-acceleration history of the artificial earthquake GEQ II. (After Abdel-Motaal, 1999)

Figures 9, 10 & 11 show the effect of the foundation type on the periodic time of the structure, the absolute peak acceleration, and displacement at the top level of the building, respectively. The foundation type has a significant positive effect on the building's seismic response with a general note that the raft solution is practically close to the results of isolated footings connected with rigid concrete ties.

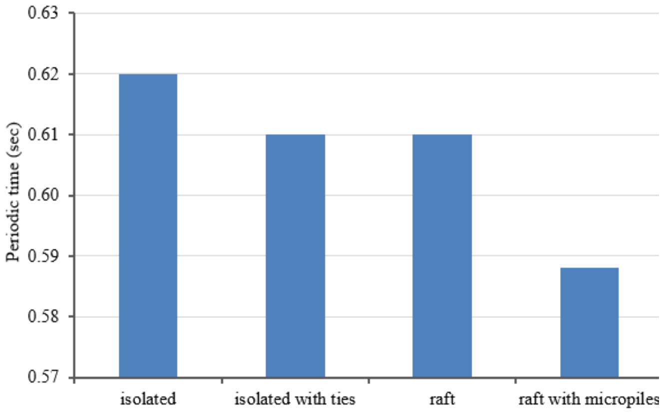

Fig.9: Periodic time of the building considering various foundation types.

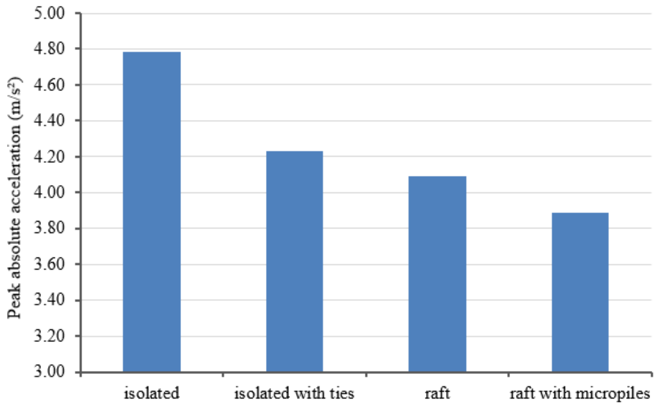

Fig.10: Peak absolute acceleration at building top level, considering various foundation types.

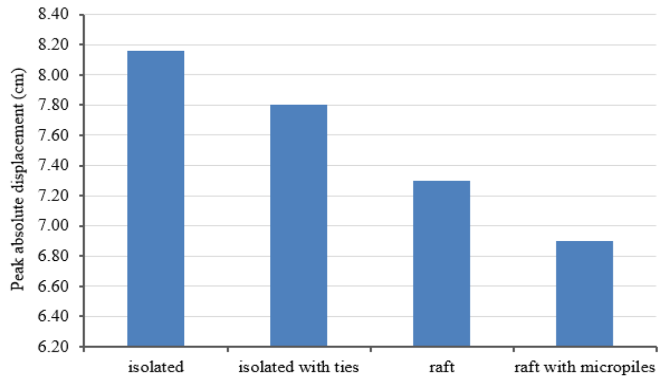

Fig.11: Peak absolute horizontal displacement at building top level, considering various foundation types.

B. Effect of micropiles structure

Free field analysis is done to study the behavior of seismic waves throughout its way, along with the soil layers. Initially, the effect of GEQ II earthquake accelerations is investigated by analyzing the same model without application of any structure at different four cases of absolute peak acceleration for the earthquake 0.04g, 0.08g, 0.12g, and 0.16g. The peak absolute acceleration values at several levels are plotted versus the total depth of the soil column, as shown in Fig.12. It is noted that the waves' acceleration has been amplified almost along all the soil column. It should be mentioned that other soil layers may achieve attenuation behavior.

As recommended by the design codes in Egypt, the peak acceleration level is taken within a range of 0.1 to 0.2 g at the foundation level. So, the whole next parametric study will be taken with earthquake GEQ II scaled to get acceleration around 0.2g at the foundation level as interpolated in Fig.13 (i.e. peak acceleration at bedrock level is selected = 0.72 m/s^2). The following sections aim to study the effect of micropiles length, diameter, and number on the seismic response of the structure.

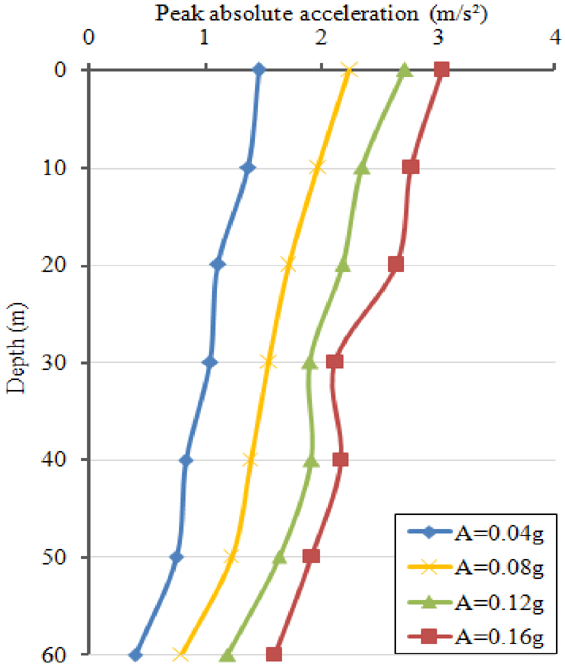

Fig.12: Relation between peak absolute acceleration and the total depth of soil column at free field case.

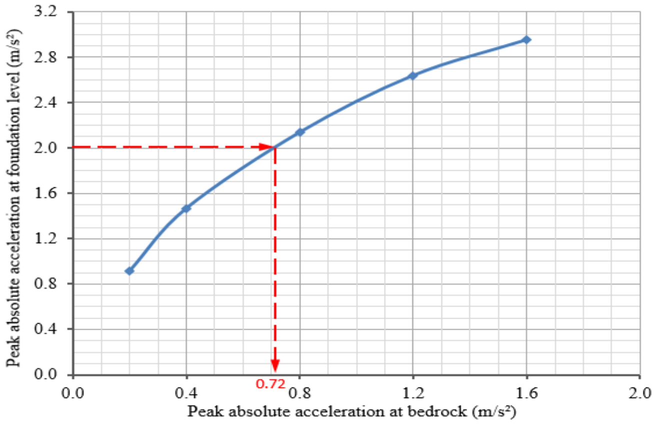

Fig.13: Interpolation of the required earthquake peak acceleration.

(1) Effect of micropile length

Figures 14 & 15 show the absolute peak acceleration and horizontal displacement values at the highest level of the ten-story building and Fig.16 shows the absolute maximum bending moment along the micropile for different lengths of micropiles with the same proposed micropile diameter 25 cm and with micropiles configuration gives 18 micropiles at one uniform span of the building. These relations were investigated for pile lengths 7, 10, 15, 21 (the proposed length), and 25m at two cases for the top clayey SILT and SAND soil layer considering G = 40 & 100 MPa. Zero pile length means a shallow raft foundation without micropiles.

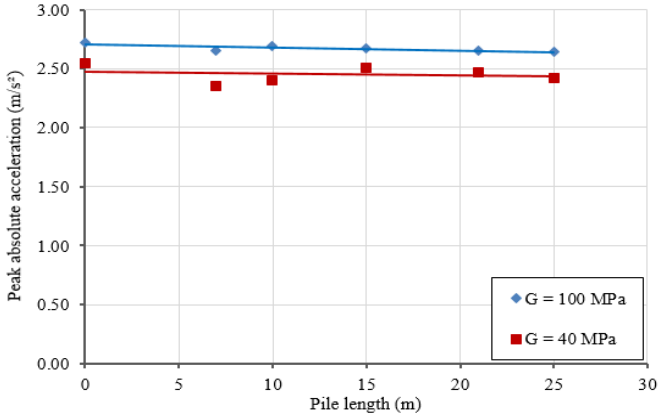

Fig.14: Peak absolute acceleration at the highest level of the ten-story building considering different micropile lengths.

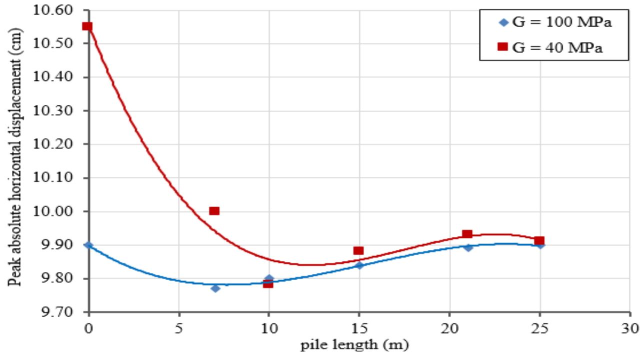

Fig.15: Peak absolute horizontal displacement at the highest level of the ten-story building considering different micropile lengths.

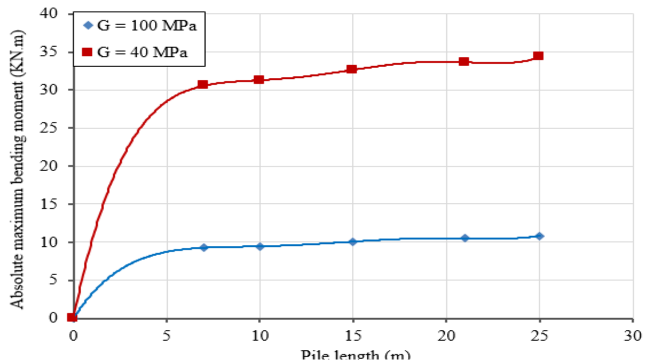

Fig.16: Absolute maximum bending moment along the micropile considering different micropile lengths

The following could be established:

1. Micropile length effect on acceleration and horizontal displacement values have a limited or insignificant effect due to the resulting double effect, as it leads to an increase in foundation fixation as well as an increase in the pile's buckling ratio.
2. The peak absolute bending moment is directly proportional to the pile length in a relatively nonlinear behavior. Micropile length has a significant impact on the values of the bending

Published By:
Blue Eyes Intelligence Engineering
and Sciences Publication

moment and the stability of the micropile itself.

3. Bending moment values increase by about 17% and 13% in cases of shear modulus for the top layer with 100 MPa and 40 MPa, respectively, when the micropile length increases from 7 to 25 meters. It should be mentioned that the moment increases by 13% has a more dramatic effect in the case of shear modulus for the top layer with 40 MPa because it exceeds the structural capacity of the micropile cross-sectional area. On the other hand, the increase of bending moment in the case of shear modulus for the topsoil layer with 100 MPa by 17% has a very restricted effect, as the value of bending moment is small relative to the structural capacity of the micropile cross-section.
4. Bending moment values are less in case of high stiffness top layer with around 330 % than the values in case of low stiffness topsoil layer, which clarifies the importance of compaction of the surface soil layer before construction in seismically active zones.

(2) Effect of micropile diameter

Figures 17 & 18 show the absolute peak acceleration and horizontal displacement values at the highest level of the ten-story building, respectively. In contrast, Fig.19 shows the absolute maximum bending moment along the micropile for different diameters of micropiles with the same proposed micropile length 21 m and with the same micropiles configuration, which gives 18 micropiles at one uniform span of the building. These relations were investigated for pile diameters 0.15, 0.25 (the proposed diameter), and 0.35 m considering the same two cases for the topsoil layer. Zero pile length means a shallow raft foundation without micropiles. The following could be established:

1. The absolute peak acceleration and horizontal displacement values decrease moderately with the increase in the micropile diameter. Micropile diameter has a moderately positive effect on increasing the efficiency of foundation fixation of the building, especially for the case of weak topsoil conditions.
2. The peak absolute bending moment is directly proportional to the micropile diameter in a relatively nonlinear behavior, which is returned to the increase of the width of the active wedge (lateral loads) acting on the pile and the increase of pile's flexural rigidity.
3. Bending moment values are less in case of high stiffness top layer with around 330 % than the values in case of low stiffness top layer. Also, as noticed in Fig.18, the effect of the increase in micropile diameter is more evident in the case of low stiffness topsoil layer.

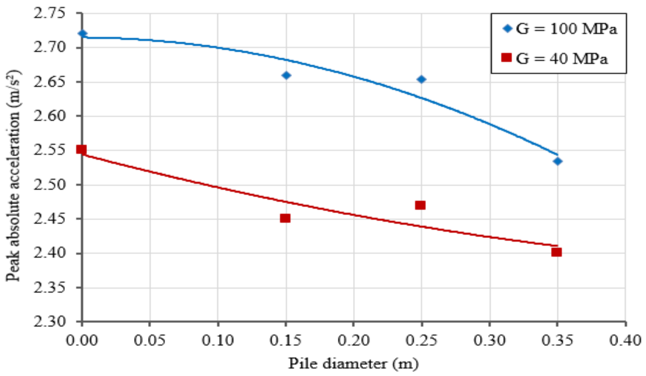

Fig.17: Peak absolute acceleration at the highest level of the ten-story building considering different micropile diameters.

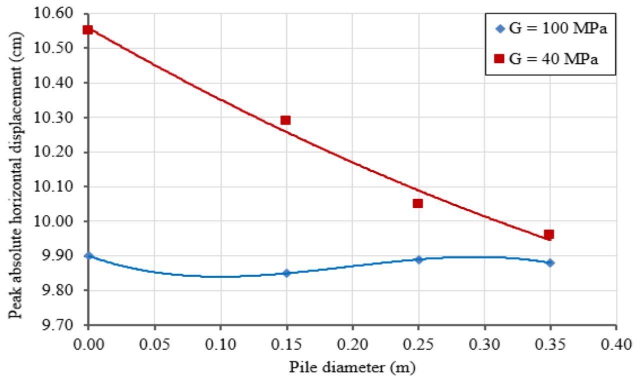

Fig.18: Peak absolute horizontal displacement at the highest level of the ten-story building considering different micropile diameters.

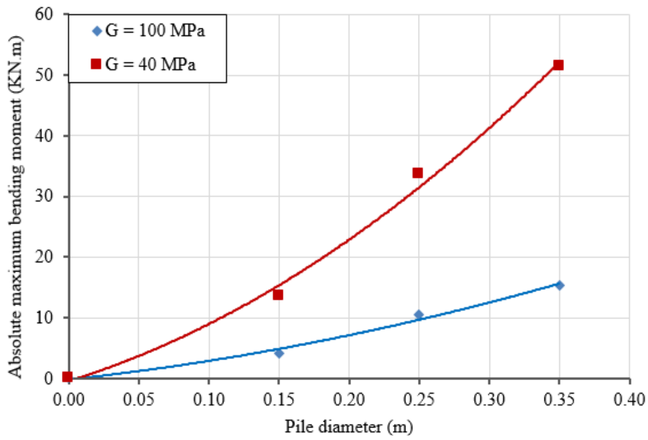

Fig.19: Absolute maximum bending moment along the micropile considering different micropile diameters.

(3) Effect of number of micropiles

Figures 20 & 21 show the absolute peak acceleration and horizontal displacement values at the highest level of the ten-story building, respectively. Fig.22 shows the absolute maximum bending moment along the micropile for different configurations of micropiles with the firstly proposed micropile length and diameter with 21 m and 25 cm, respectively. These relations were investigated for various numbers of micropiles in every strip of the uniform studied structure, estimated with 18 (the proposed distribution), 34, and 46 considering the same topsoil layers.

The following could be established:

1. The absolute peak acceleration and horizontal displacement values decrease with the increase in the number of micropiles. The number of micropiles has a positive effect on increasing foundation fixation efficiency.
2. As illustrated in Fig.22, the increase in the used number of micropiles led to a significant decrease in bending moment along micropiles length as predicted. It could be clarified as the total moment will be divided on a higher number of piles, and hence moment per single pile will decrease.
3. Bending moment values are less in case of high stiffness top layer with around 280 % than the values in case of low stiffness top layer, which clarifies the importance of compaction of the surface soil layer before construction in seismically active areas.

Retrieval Number: F1511089620/2020©BEIESP
DOI: 10.35940/ijeat.F1511.089620
Journal Website: www.ijeat.org

Published By:
Blue Eyes Intelligence Engineering
and Sciences Publication

4. The curves shape reflects the importance of carrying extensive study for selecting the economic number of piles. This number is inversely proportional to the stiffness of the top layer. For more clarification, it may be evident that 25 piles may be an efficient and economical number of piles in the case of the topsoil layer having G = 40 MPa, as clarified in Fig. 21.
5. As a general note in the study of micropiles parameters (length, diameter, and number), the absolute maximum acceleration values are higher in case of high stiffness top layer unexpectedly. This may be returned to the relation between the whole soil column frequency compared with the structure's frequency that may affect waves' attenuation and amplification.

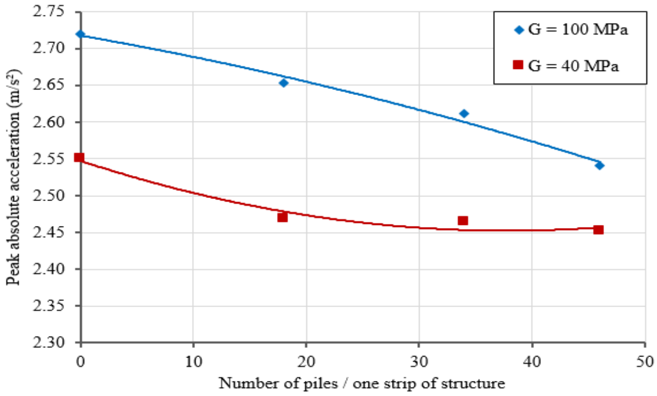

Fig.20: Peak absolute acceleration at the highest level of the ten-story building in different cases of the used number of micropiles.

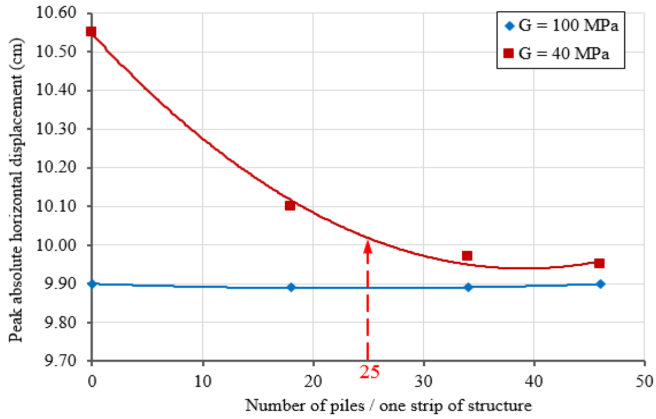

Fig.21: Peak absolute horizontal displacement at the highest level of the ten-story building in different cases of the used number of micropiles.

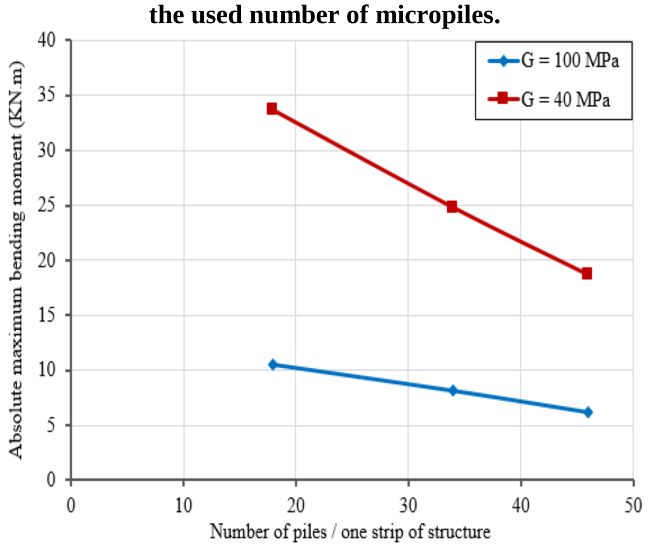

Fig.22: Absolute maximum bending moment along the micropile in different cases of the used number of micropiles.

C. Effect of Floors number (Mass of Superstructure)

Structure properties have a considerable influence on the seismic performance of buildings. Therefore, the representation of the whole structure is more accurate than the modeling of the superstructure with a single degree of freedom system. In this section, the influence of the frequency of the superstructure (periodic time) on its response is studied. Figure 23 shows the used PLAXIS 2D model to simulate the cases of different numbers of building stories (two, four, seven, ten, and fifteen stories). The difference in the number of building stories expresses about two effects, namely changing the mass of the superstructure as well as the difference in the structure height. The structure is founded on the same described soil layers, which their properties are illustrated in Table-I, and with the same proposed micropiles, under the effect of the same earthquake with a peak acceleration of 0.72 m/s^2.

Figure 24 shows the periodic time of the structure with the difference in the number of stories. This relationship is typically approximated by 0.1 × the number of floors. Also, the periodic time of the building is determined from the numerical model analysis in cases of raft foundation only and raft with micropiles. The periodic time for the case of the raft foundation is larger than the case of a raft with micropiles. This may be a result of the increase in the building's stiffness with the addition of the micropiles. The maximum absolute bending moment and shear force at the middle micropile are shown in Figs. 25& 26 respectively to study the micropiles' response. Maximum values are recorded at the micropile head in all structure cases.

Also, Figures 27 and 28 show the peak absolute acceleration and horizontal displacement values at the highest level of the structure. The recorded values of the acceleration and displacement are at different levels due to the height difference. The drift for the whole building is calculated in each case, as indicated in Fig. 29, where the drift is the ratio between the peak absolute horizontal displacements difference and building height. The following is noted:

1. Peak values are recorded in the cases of the number of floors in the range of three and eight floors; then the values are in noticeable decrease, then in a nonlinear continuous increase which is expected to increase at a very high number of floors more than the peak values illustrated in curves. The reasons for that could be the double effect of the superstructure mass, and the relationship between the fundamental periodic time of the superstructure and the dynamic characteristics of the seismic waves at the foundation level.
2. By examining the peak response spectrum curve (PSA) at the foundation level, as shown in Fig. 30, it is clear that its values are almost the same in all cases of the number of stories of the superstructure, it is found that peak value is at periodic time equals 0.67 sec. By comparing this result with the maximum magnification shown in Figs 25 through 28, which is found around six number of floors.

Retrieval Number: F1511089620/2020©BEIESP
DOI: 10.35940/ijeat.F1511.089620
Journal Website: www.ijeat.org

Published By:
Blue Eyes Intelligence Engineering
and Sciences Publication

3. The fundamental periodic time at six number of floors can be estimated with 0.77 sec from Fig. 24, which clarifies that the maximum magnification occurred due to approaching the maximum amplification zone (fundamental periodic time nearly equal to the dominant periodic time of the seismic waves).
4. Fig. 30 illustrates the peak response spectrum at the foundation level in different cases, considering the average envelope for the response spectrum it will be like the common shape of the normalized response spectrum illustrated in Fig. 31, which is the normalized response spectrum of the 1994 UNIFORM building code 27. It should be mentioned that the concluded average envelope response spectrum is like a case between soil types 2 and 3 as predicted from the soil's formation in the studied problem.
   It is evident that after periodic time around 0.8 sec, a zone of low spectral values is shown, and the influencing factor is the mass of superstructure. This note explains the re-increase in all values after ten floors case, which could be considered as a transfer zone where the mass is not very high, and the fundamental periodic time is out of peak spectral values zone.
5. These conclusions are not constant for all cases as it depends on the type of soil and peak response spectrum of the earthquake itself. So, the peak spectral values zone may differ, and thus the maximum amplification will occur at a different floor number or different building height. This makes the study of each case separately with highlighting the role of soil type an important matter in design and determination of the number of the used micropiles and even in superstructure design.

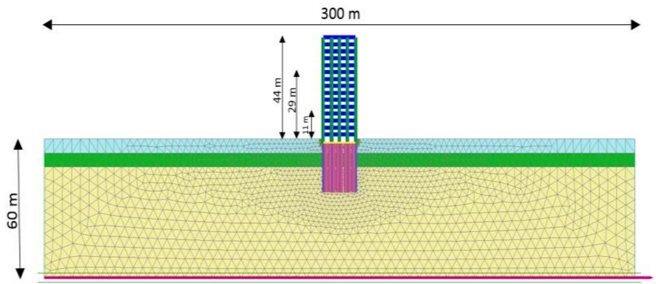

Fig.23: They PLAXIS 2D model to simulate the cases of a different number of building stories.

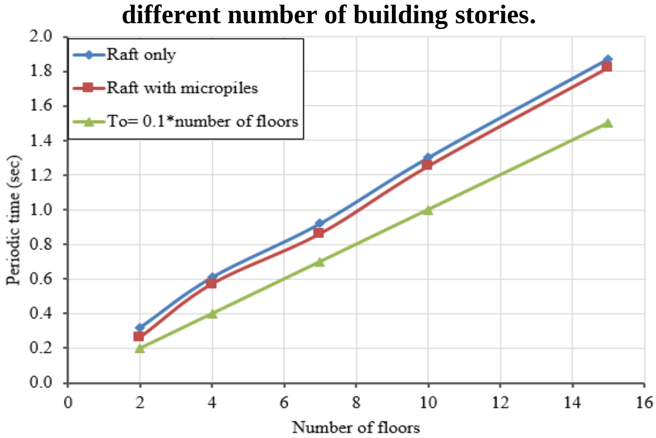

Fig.24: Relation between the number of building's floors and its periodic time.

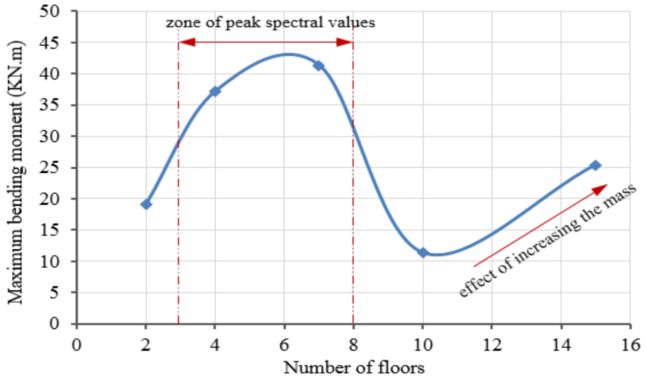

Fig. 25: Relation between the number of building's floors and the maximum absolute bending moment at the middle micropile.

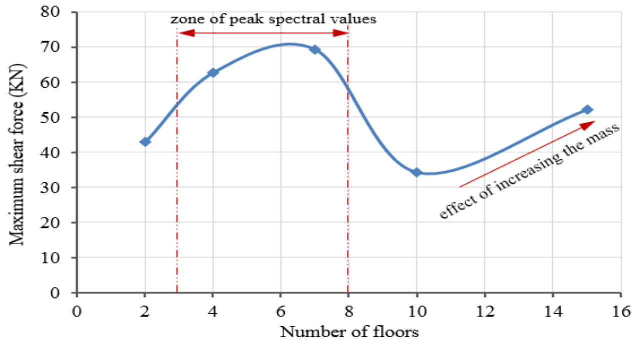

Fig. 26: Relation between the number of building's floors and the maximum absolute shear force at the middle micropile.

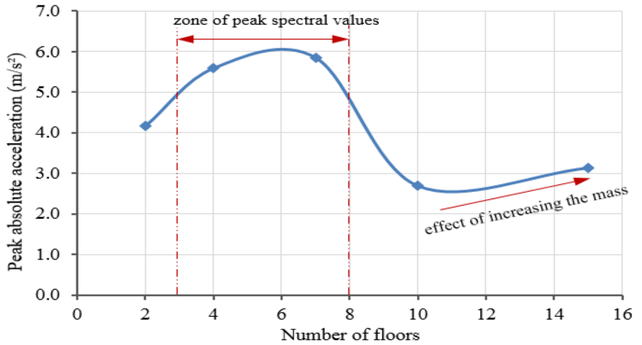

Fig. 27: Relation between the number of building's floors and the peak absolute acceleration at the highest level of the building.

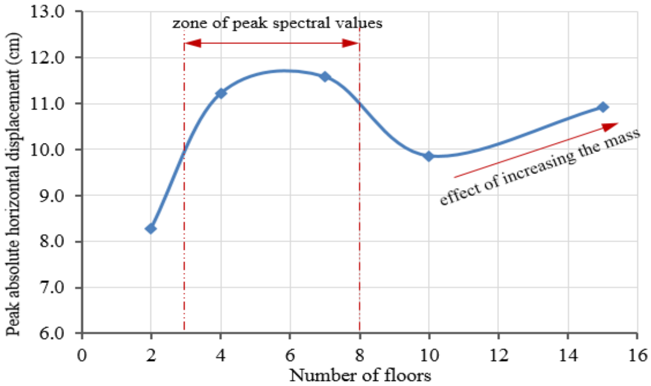

Fig. 28: Relation between the number of building's floors and the resulted peak absolute horizontal displacement at the highest level of the building.

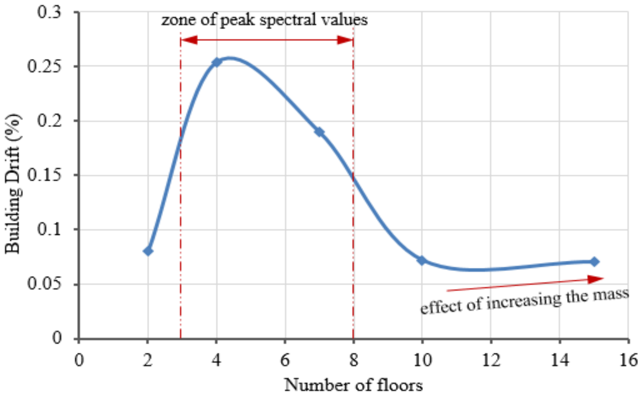

Fig. 29: Relation between the number of building's floors and the whole building drift value.

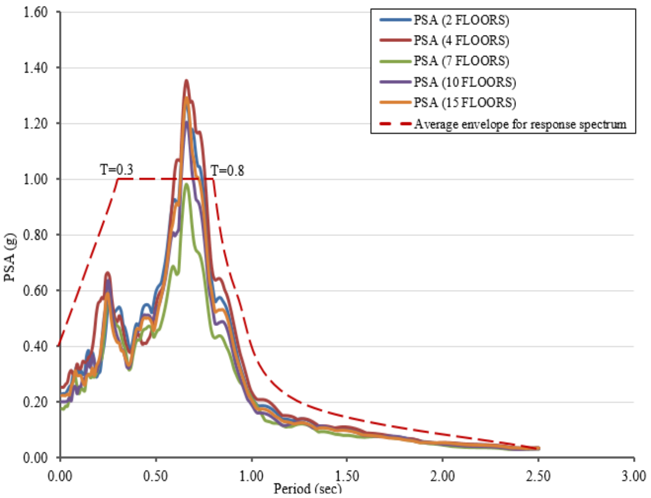

Fig. 30: Peak response spectrum at the foundation level by analysis of different cases of stories number.

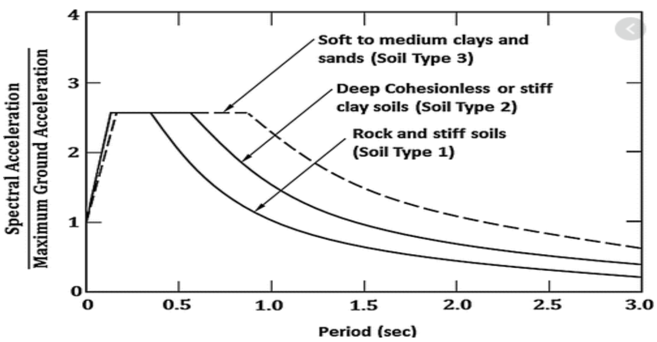

Fig. 31: Normalized Response spectra shapes for different soil conditions. (quoted from UBS, 1994)

VI. CONCLUSIONS

The following conclusions can be drawn from this research:

1. Seismic response analysis considering several foundation types (shallow and deep foundations) shows that the stiffness of the foundation has a significant effect on the building's seismic response with a general note that the raft foundation behavior is close to the behavior of isolated footings connected with rigid reinforced concrete ties.
2. With increase micropile length, the micropile peak absolute bending moment increases proportionally to the micropile length in a relatively nonlinear behavior. Micropile length effect can be considered a limited effect due to the resulting double effect, as it leads to an increase in foundation fixation as well as an increase in pile's buckling ratio.
3. With increase micropile diameter, the resulted peak absolute acceleration and horizontal displacement values decrease moderately. While the micropile peak absolute bending moment increases proportionally to the micropile diameter in a relatively nonlinear behavior, which is returned to the increase of the width of the active wedge acting on the micropile, which causes an increase for lateral loads.
4. By increasing the number of micropiles, the resulted peak absolute acceleration and horizontal displacement values decrease moderately. While the micropile peak absolute bending moment decreases significantly. Results reflected the importance and capability of selecting the economic number of piles, which is inversely proportional to the stiffness of the topsoil layer.
5. Bending moment acting on micropiles are less in case of high stiffness base layer to about one-third of the values in case of low stiffness base layer which clarifies the effectiveness of compaction of the surface soil layer before construction in seismically active zones and the importance of using micropiles if compaction is not applicable.
6. Seismic response analysis of the main structure with different number of floors reveals the following,
   a) Different numbers of floors achieve a double effect, which is the superstructure mass and the relation between the periodic time of the superstructure and the underlying soil. Peak values are recorded in the case of building with six floors as its periodic time is very close to the periodic time of the whole soil column, which clarifies that this maximum magnification occurred due to resonance phenomenon.
   b) These conclusions are not constant in all cases as it depends on the type of soil and peak response spectrum of the earthquake itself. So the peak spectral values zone may differ, which makes the study of each case separately with highlighting the role of soil type as a vital matter in the design and determination of the number of the used micropiles as well as in superstructure design.

VII. NOTATIONS

α	Rayleigh co-efficient
β	Rayleigh co-efficient
$\gamma_{0.7}$	Shear strain threshold
υ_{ur}	unloading-reloading Poisson's ratio
ξ	Soil damping ratio [%]
σ_3	Minor effective principal stress [kN/m^2]
φ	Friction angle [°]
ω	Angular frequency [rad]
E^{ref}	Reference soil young's modulus [MPa]
E_{ur}^{ref}	Reference unloading-reloading stiffness [MPa]
g	Gravity acceleration
G_o^{ref}	Small strain shear modulus [MPa]
P_{ref}	Reference confining pressure [MPa]
V_s	Shear wave velocity [m/s^2]

Retrieval Number: F1511089620/2020©BEIESP
DOI: 10.35940/ijeat.F1511.089620
Journal Website: www.ijeat.org

Published By:
Blue Eyes Intelligence Engineering
and Sciences Publication

REFERENCES

1. Kramer, S. L., and others. (1996). *Geotechnical earthquake engineering*. Pearson Education India.
2. Reese, L. C. (2001). "Van Impe." *WF, Single Piles and Pile Groups Under Lateral Loading, AA Balkema, Rotterdam*.
3. O'Rourke, T. D., Meyersohn, W. D., Shiba, Y., Chaudhuri, D., and others. (1994). "Evaluation of pile response to liquefaction-induced lateral spread." *Proc., 5th US-Japan Workshop on Earthquake Resistant Design of Lifeline Facilities and Countermeasures Against Soil Liquefaction*, 457–478.
4. Bhattacharya, S., Madabhushi, S. P. G., and Bolton, M. D. (2004). "An alternative mechanism of pile failure in liquefiable deposits during earthquakes." *Geotechnique*, Thomas Telford Ltd, 54(3), 203–213.
5. Seed, H. B. (1970). "Whitman." *RV, Design of Earth Retaining Structures for Dynamic*.
6. Ishibashi, I., and Zhang, X. (1993). "Unified dynamic shear moduli and damping ratios of sand and clay." *Soils and foundations*, The Japanese Geotechnical Society, 33(1), 182–191.
7. Sharma, B., Hussain, Z., and others. (2019). "Behaviour of Batter Micropiles Subjected to Vertical and Lateral Loading Conditions." Journal of Geoscience and Environment Protection, Scientific Research Publishing, 7(02), 206.
8. Matlock, H., and Reese, L. C. (1962). "Generalized solutions for laterally loaded piles." *Transactions of the American Society of Civil Engineers*, ASCE, 127(1), 1220–1247.
9. McClelland, B., and others. (1956). "Soil modulus for laterally loaded piles." *Journal of the Soil Mechanics and Foundations division*, ASCE, 82(4), 1–22.
10. Higgins, W., Martindale, H., Chakraborty, T., and Basu, D. (2010). "Assessment of the PY method for laterally loaded pile in sand." Indian Geotechnical conference, 833–836.
11. Wong, J. C. (2004). "Seismic behavior of micropiles."
12. Toma, M. A. (2017). "Earthquake Response Analysis of Pile Supported Structures-Correspondence of PLAXIS 2D with Eurocode 8." NTNU.
13. Shahrour, I., and Juran, I. (2004). "Seismic behaviour of micropile systems." *Proceedings of the Institution of Civil Engineers-Ground Improvement*, Thomas Telford Ltd, 8(3), 109–120.
14. Alsaleh, H., Shahrour, I., and Souli, M. (2011). "3D elastoplastic analysis of the seismic performance of inclined micropiles."
15. Ghorbani, A., Hasanzadehshooiili, H., Ghamari, E., and Medzvieckas, J. (2014). "Comprehensive three dimensional finite element analysis, parametric study and sensitivity analysis on the seismic performance of soil--micropile-superstructure interaction." *Soil Dynamics and Earthquake Engineering*, Elsevier, 58, 21–36.
16. Alfach, M. T. (2019). "Reinforcement the Seismic Interaction of Soil-Damaged Piles-Bridge by Using Micropiles." International Workshop on Simulation Science, 179–195.
17. Mashhoud, H. J., Yin, J.-H., Panah, A. K., and Leung, Y. F. (2020). "A 1-g shaking table investigation on response of a micropile system to earthquake excitation." Acta Geotechnica, Springer, 15(4), 827–846.
18. Benz, T. (2007). *Small-strain stiffness of soils and its numerical consequences*. Univ. Stuttgart, Inst. f. Geotechnik Stuttgart.
19. Obrzud, R. (2011). "The Hardening Soil model with small strain stiffness." Lausanne: GeoMod SA.
20. Vucetic, M., and Dobry, R. (1991). "Effect of soil plasticity on cyclic response." Journal *of geotechnical engineering*, American Society of Civil Engineers, 117(1), 89–107.
21. Hardin, B. O., and Black, W. (1969). "Closure on vibration modulus of normally consolidated clay." *Journal of Soil Mechanics & Foundations Div*.
22. Chopra, A. K. (2007). "Earthquake Spectra." *Dynamics of Structures—Theory and Applications to Earthquake Engineering (3rd ed.). New Jersey: Prentice-Hall*.
23. Versions, P. (2004). "Scientific material models dynamic manual/RBY Brink-greve, W. Breere." *Delft University of Technology Plaxis bv, The Netherlands*.
24. Rahmani, A., Taiebat, M., Finn, W. D. L., and Ventura, C. E. (2018). "Evaluation of py springs for nonlinear static and seismic soil-pile interaction analysis under lateral loading." *Soil Dynamics and Earthquake Engineering*, Elsevier, 115, 438–447.
25. Thapa Magar, A. (2016). "Earthquake Response of Different Types of Retaining Walls." NTNU.
26. Abdel-Motaal, M. (1999). "Soil effect on the dynamic behavior of framed structures." Ph. D. Thesis, Faculty of Engineering, University of Ain Shams, Cairo.
27. Code, U. B. (1994). "1997." *International Building Office, Whittier, California*.

AUTHORS PROFILE

Noha El-Shamy is a demonstrator of geotechnical engineering at Ain Shams University, Cairo, Egypt. She is currently doing her M.Sc. in geotechnical engineering, civil engineering department. She obtained her B.Sc. degree (2017) in civil engineering from Ain Shams University. Her research interests are in Dynamic soil behavior, earthquakes, soil-structure interaction and numerical modelling. She has a wide experience by the design and construction of different shallow and deep foundations as well as various earth-supporting systems through participating in many geotechnical projects in Egypt and Saudi Arabia. She was also involved in many projects dealing with earth dams and ground improvement.

Sayed M. Ahmed is an associate professor in Geotechnical Engineering at Ain Shams University of Engineering. He graduated with a Ph.D. from Ain Shams University, Egypt, in 2001. He has broad experience in geotechnical engineering academic and professional works. His main interests are in the soft-ground tunneling, deep excavations, and in-situ-testing. Through more than 25 years of practical and academic work, he has a wide experience in teaching, design and analysis of different geotechnical systems in several countries including Egypt and Saudi Arabia. He has published many research articles in peer-reviewed international journals and conferences dealing with different geotechnical topics.

M. A. Abdel-Motaal is a professor in geotechnical Engineering. He graduated with a Ph.D. from Ain Shams University, Egypt, in 1999. He has been a researcher and consultant for over 20 years. He also has been a member of referee committee of the Journal of the Egyptian Engineers Society, Faculty of Engineering, Cairo University since 2018, Faculty of Engineering, Ain Shams University and director of Soil Mechanics and Foundation Research Unit (SMFU), Faculty of Engineering, Ain Shams University (April, 2012 and till 2016). He has supervised several MSC and PhD Theses. He has been a consultant for many Geotechnical projects and Participated in many Engineering conferences and has a publications list exceeding 20 Papers in Different Engineering Journals.

Retrieval Number: F1511089620/2020©BEIESP
DOI: 10.35940/ijeat.F1511.089620
Journal Website: www.ijeat.org

Published By:
Blue Eyes Intelligence Engineering and Sciences Publication